

# Precise measurements of the $\eta$ meson and the neutral kaon masses with the KLOE detector

The KLOE collaboration

F. Ambrosino,<sup>d</sup> A. Antonelli,<sup>a</sup> M. Antonelli,<sup>a</sup> F. Archilli,<sup>a</sup> C. Bacci,<sup>g</sup> P. Beltrame,<sup>b</sup> G. Bencivenni,<sup>a</sup> S. Bertolucci,<sup>a</sup> C. Bini,<sup>f</sup> C. Bloise,<sup>a</sup> S. Bocchetta,<sup>g</sup> F. Bossi,<sup>a</sup> P. Branchini,<sup>g</sup> R. Caloi,<sup>f</sup> P. Campana,<sup>a</sup> G. Capon,<sup>a</sup> T. Capussela,<sup>a</sup> F. Ceradini,<sup>g</sup> S. Chi,<sup>a</sup> G. Chiefari,<sup>d</sup> P. Ciambrone,<sup>a</sup> E. De Lucia,<sup>a</sup> A. De Santis,<sup>f</sup> P. De Simone,<sup>a</sup> G. De Zorzi,<sup>f</sup> A. Denig,<sup>b</sup> A. Di Domenico,<sup>f</sup> C. Di Donato,<sup>d</sup> B. Di Micco,<sup>g\*</sup> A. Doria,<sup>d</sup> M. Dreucci,<sup>a\*</sup> G. Felici,<sup>a</sup> A. Ferrari,<sup>a</sup> M. L. Ferrer,<sup>a</sup> S. Fiore,<sup>f</sup> C. Forti,<sup>a</sup> P. Franzini,<sup>f</sup> C. Gatti,<sup>a</sup> P. Gauzzi,<sup>f</sup> S. Giovannella,<sup>a</sup> E. Gorini,<sup>c</sup> E. Graziani,<sup>g</sup> W. Kluge,<sup>b</sup> V. Kulikov,<sup>j</sup> F. Lacava,<sup>f</sup> G. Lanfranchi,<sup>a</sup> J. Lee-Franzini,<sup>ah</sup> D. Leone,<sup>b</sup> M. Martini,<sup>a</sup> P. Massarotti,<sup>d</sup> W. Mei,<sup>a</sup> S. Meola,<sup>d</sup> S. Miscetti,<sup>a</sup> M. Moulson,<sup>a</sup> S. Müller,<sup>a</sup> F. Murtas,<sup>a</sup> M. Napolitano,<sup>d</sup> F. Nguyen,<sup>g</sup> M. Palutan,<sup>a</sup> E. Pasqualucci,<sup>f</sup> A. Passeri,<sup>g</sup> V. Patera,<sup>ae</sup> F. Perfetto,<sup>d</sup> M. Primavera,<sup>c</sup> P. Santangelo,<sup>a</sup> G. Saracino,<sup>d</sup> B. Sciascia,<sup>a</sup> A. Sciubba,<sup>ae</sup> A. Sibidanov,<sup>a</sup> T. Spadaro,<sup>a</sup> M. Testa,<sup>f</sup> L. Tortora,<sup>g</sup> P. Valente,<sup>f</sup> G. Venanzoni,<sup>a</sup> R. Versaci<sup>a</sup> and G. Xu<sup>ai</sup>

<sup>a</sup>Laboratori Nazionali di Frascati dell'INFN, Frascati, Italy

<sup>b</sup>Institut für Experimentelle Kernphysik, Universität Karlsruhe, Germany

<sup>c</sup>Dipartimento di Fisica dell'Università e Sezione INFN, Lecce, Italy

<sup>d</sup>Dip. di Scienze Fisiche dell'Università "Federico II" e Sezione INFN, Napoli, Italy

<sup>e</sup>Dipartimento di Energetica dell'Università "La Sapienza", Roma, Italy

<sup>f</sup>Dipartimento di Fisica dell'Università "La Sapienza" e Sezione INFN, Roma, Italy

<sup>g</sup>Dipartimento di Fisica dell'Università "Roma Tre" e Sezione INFN, Roma, Italy

<sup>h</sup>Physics Department, State University of New York at Stony Brook, U.S.A.

<sup>i</sup>Institute of High Energy Physics of Academia Sinica, Beijing, China

<sup>j</sup>Institute for Theoretical and Experimental Physics, Moscow, Russia

E-mail: dimicco@fis.uniroma3.it, marco.dreucci@lnf.infn.it

ABSTRACT: We present precise measurements of the  $\eta$  and  $K^0$  masses using the processes  $\phi \rightarrow \eta\gamma$ ,  $\eta \rightarrow \gamma\gamma$  and  $\phi \rightarrow K_S K_L$ ,  $K_S \rightarrow \pi^+\pi^-$ . The  $K^0$  mass measurement,  $M_K = 497.583 \pm 0.005_{\text{stat}} \pm 0.020_{\text{syst}}$  MeV, is in acceptable agreement with the previous measurements but is more accurate. We find  $m_\eta = 547.874 \pm 0.007_{\text{stat}} \pm 0.029_{\text{syst}}$  MeV. Our value is the most accurate to date and is in agreement with two recent measurements based on  $\eta$  decays, but is inconsistent, by about  $10\sigma$ , with a measurement of comparable precision based on  $\eta$  production at threshold.

KEYWORDS: e+e- Experiments.

\*Corresponding author.

---

## Contents

|   |           |
|---|-----------|
| <b>1. Introduction</b>                          | <b>1</b>  |
| <b>2. The KLOE experiment</b>                   | <b>1</b>  |
| <b>3. Calibration of c.m. energy</b>            | <b>2</b>  |
| <b>4. Measurement of the neutral kaon mass.</b> | <b>3</b>  |
| <b>5. The <math>\eta</math> mass</b>            | <b>6</b>  |
| <b>6. Conclusions</b>                           | <b>11</b> |

---

## 1. Introduction

The  $\eta$ -meson mass has changed four times in the past 40 years while the measuring accuracy never was better than 0.15 MeV till 2002. In 2005 the GEM experiment using the reaction  $d + p \rightarrow \eta \ ^3\text{He}$  at threshold found  $m_\eta = (547.311 \pm 0.028_{\text{stat}} \pm 0.032_{\text{syst}})$  MeV [1], while in 2002 the NA48 collaboration using the decay  $\eta \rightarrow \pi^0 \pi^0 \pi^0$  found  $m_\eta = (547.843 \pm 0.030_{\text{stat}} \pm 0.041_{\text{syst}})$  MeV [2]. The two results above differ by about eight standard deviations. Preliminary KLOE results [3]  $m_\eta = (547.822 \pm 0.005_{\text{stat}} \pm 0.069_{\text{syst}})$  confirm the disagreement. Recently the CLEO-c collaboration found  $m_\eta = (547.785 \pm 0.017_{\text{stat}} \pm 0.057_{\text{syst}})$  MeV [4] using  $\psi(2S) \rightarrow \eta J/\psi$  decays and combining different decay modes of the  $\eta$ .

For the  $K^0$  mass there is good agreement between the Novosibirsk (1995) and CERN (2002) measurements that have a precision of  $\sim 30$  keV [5, 6]. Our measurement, similar to that of Novosibirsk with rather increased statistics, is based on the knowledge of the  $\phi$  meson mass which is known to 20 ppm from the Novosibirsk measurement employing the g-2 depolarizing resonance method. The  $\phi$  mass is also the basis for the  $\eta$  mass measurement which relies on a precise determination of the collision center of mass energy,  $W$  in the following.  $W$  is determined run by run using  $e^+e^- \rightarrow e^+e^-$  events ( $\sim 40,000$  for each run), while the absolute momentum scale is obtained from the  $e^+e^- \rightarrow \phi \rightarrow K_S K_L$  cross section as a function of  $W$ .

## 2. The KLOE experiment

KLOE operates at DAΦNE, the  $\phi$ -factory  $e^+e^-$  collider running at a center of mass  $W$  equal to the  $\phi$ -meson mass. Positrons and electrons collide at an angle of  $\pi - 0.025$  rad. The KLOE detector consists of a 4 m diameter, 3.2m length drift chamber, DC [7], surrounded by a lead/scintillating-fiber sampling calorimeter, EMC [8], both immersed in a

axial magnetic field of 0.52 T with the axis parallel to the bisectrix of the two beam lines. The transverse momentum resolution for charged particles is  $\delta p_{\perp}/p_{\perp} \simeq 0.4\%$ . The EMC consists of a barrel and two end caps. Energy deposits in the EMC are reconstructed in the calorimeter with energy and time resolutions  $\sigma_E/E = 0.057/\sqrt{E}$  (GeV),  $\sigma_t = 54$  ps /  $\sqrt{E}$  (GeV) added in quadrature with 140 ps. The centroid of showers is measured with resolution  $\sigma_{\ell} = 1$  cm/ $\sqrt{E}$  (GeV) in the coordinate parallel to the fibers and 1 cm in the transverse coordinate.

For a photon coming from the IP the angular resolution is  $\sigma \sim 1\text{cm}/200\text{cm} \sim 5$  mrad. Close-by energy deposits are combined into “clusters”. A prompt photon is defined as a cluster with  $|t_{\text{clu}} - r_{\text{clu}}/c| < 5\sigma_t$  ( $t_{\text{clu}}$  is the arrival time measured at the EMC,  $r_{\text{clu}}$  is the distance from the  $e^+e^-$  interaction point and  $c$  is the velocity of light) not associated to a charged particle. For this latter, we require the distance between the centroid of the cluster and the extrapolation of any track reaching the calorimeter to be larger than three times the cluster position resolution.

Only calorimeter signals are used to trigger [9] events for these analyses. We require at least two energy deposits above threshold ( $E > 50$  MeV in the barrel and  $E > 150$  MeV in the end-cap). The trigger has a large time jitter with respect to the event time but is synchronized with the collider radio frequency with an accuracy of 50 ps. The time of the bunch crossing producing an event is determined off-line during event reconstruction.

The large cross section for  $e^+e^- \rightarrow \phi$ ,  $\sim 3$   $\mu\text{b}$  and for elastic  $e^+e^-$  scattering, Bhabha scattering, allows KLOE to collect large number of events, some 450,000 per hour. KLOE takes advantage of these events to maintain a running calibration of time and energy scales of its calorimeter, of the momentum and position resolution of the drift chamber, of the machine energy and beams crossing angle, and therefore of the center of mass motion, of the mean position of the interaction point and of the detector alignment.

### 3. Calibration of c.m. energy

The center-of-mass energy,  $W$ , has been measured for each run by fitting the  $e^+e^-$  invariant-mass distribution for Bhabha events to a Monte Carlo generated function, including radiative effects.

Initial state radiation (ISR), where one or both initial colliding particles radiate a photon before interacting, affects the  $e^+e^-$  collision center-of-mass energy  $W$  and therefore the final state invariant mass. ISR, which is mostly collinear to the beam, is in general not detected. MC Bhabha events were generated using the BABAYAGA event generator [10], which accounts for both final and initial state radiation.

An example of this fit is shown in figure 1. In a typical run, an integrated luminosity of  $50$   $\text{nb}^{-1}$  is collected and  $W$  is measured with a statistical accuracy of  $\sim 3$  keV. The stability of the momentum calibration has been studied measuring the two-pion invariant mass in  $K_S \rightarrow \pi^+\pi^-$  decay. It is found to be stable to within 10 keV in the analyzed runs.

The center-of-mass energy scale has been calibrated by obtaining the  $\phi$  mass from a fit to the cross section measurements for the process  $e^+e^- \rightarrow \phi \rightarrow K_S K_L$ . The cross section is measured at different values of  $W$  around  $M_{\phi}$  by counting the number of  $K_S \rightarrow \pi^+\pi^-$

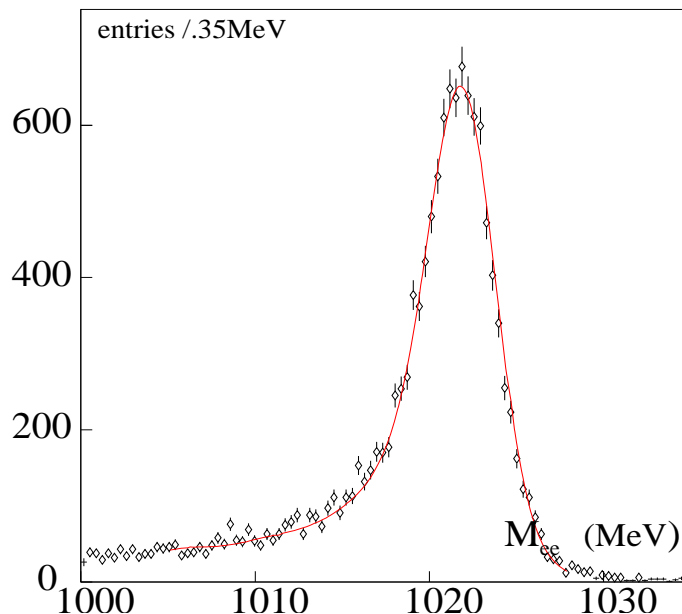


**Figure 1:** Fit to reconstructed  $e^+e^-$  invariant-mass distribution for Bhabha events, for a run with  $W=1021.7\text{MeV}$ .

events, correcting for selection efficiency, background and the  $\beta_K^3$  factor of the  $K_S K_L$  pair, and normalizing to the integrated luminosity.  $K_S \rightarrow \pi^+ \pi^-$  events are selected by requiring two tracks with opposite charge that form a vertex within a cylinder of 5 cm radius and 10 cm length centered on the interaction point. The invariant mass computed from the two pion tracks is required to be within 20 MeV of the nominal neutral kaon mass. The luminosity is measured by using very-large-angle ( $> 55^\circ$ ) Bhabha events [11].

The measured cross section is fitted to a theoretical function [12] that depends on the  $\phi$  parameters, takes into account the effect of ISR, and includes the interference with the  $\rho(770)$  and the  $\omega(782)$  mesons. The  $\phi$  mass, total width, and peak cross section are the only free parameters of the fit, the  $\rho(770)$  and the  $\omega(782)$  parameters being fixed. The results of the fit to the data are shown in figure 2. The fitted  $\phi$  mass is  $M_\phi = 1019.329 \pm 0.011$  MeV, to be compared with  $M_\phi = 1019.483 \pm 0.011 \pm 0.025$  MeV, measured by CMD-2 at VEPP-2M [13]. The ratio of these two values is used to fix the overall energy scale. The correction factor  $M_\phi^{\text{CMD}}/M_\phi^{\text{KLOE}}$  is 1.00015, corresponding to a shift in the value of  $W$  of  $\sim 150$  keV.

#### 4. Measurement of the neutral kaon mass.

The events  $\phi \rightarrow K_S K_L$  offer a unique possibility to obtain a precise value of the neutral kaon mass. To obtain a crude estimate of the resolution and explain the method used we observe that if the  $\phi$ -meson is at rest the kaon mass can be extracted from the kaon momentum using the relation:

$$m_K = \sqrt{\frac{m_\phi^2}{4} - p_K^2}; \quad \frac{\Delta m_K}{m_K} \simeq \frac{p_K^2}{m_K^2} \frac{\Delta p_K}{p_K} \sim \beta^2 \frac{\Delta p_K}{p_K} \quad (4.1)$$

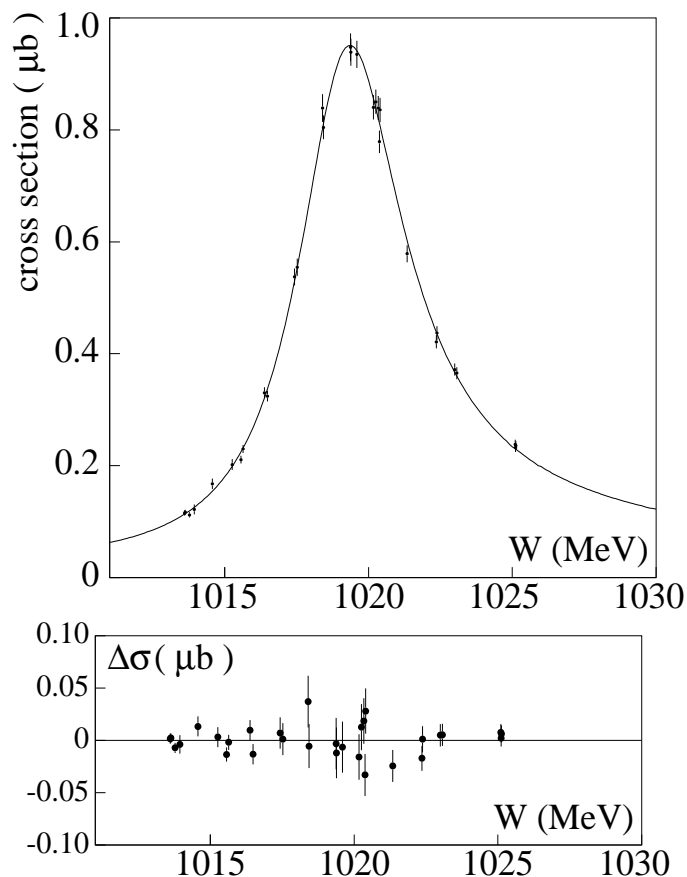


**Figure 2:** Top: Cross section for  $e^+e^- \rightarrow \phi \rightarrow K_S K_L$  as a function of the center-of-mass energy. The solid line represents the fit to the data. Bottom: Fit residuals.

Since  $p_K \simeq 110$  MeV, measuring it at 1% level, well within the KLOE capability, results in a measurement of the  $K^0$  mass better than 0.1%. 50,000 events are enough to reach a statistical accuracy of about 1 keV.

$\phi$  mesons are produced with a momentum along the  $x$  axis,  $p_\phi = 12.5$  MeV at DAΦNE. From the measured momenta of the two pions from  $K_S \rightarrow \pi^+\pi^-$ , we measure the  $K_S$  momentum. The  $K_L$  momentum is given by  $\vec{p}_{K_L} = \vec{p}_\phi - \vec{p}_{K_S}$ , where  $\vec{p}_\phi$  is the average  $\phi$  momentum measured with Bhabha events collected in the same runs. The center of mass energy of the  $K_S K_L$  pair ( $W_{KK}$ ) is related to the kaon mass  $M_K$ , according to:

$$W_{KK}(M_K) = \sqrt{2M_K^2 + 2E_{K_S}E_{K_L} - 2\vec{p}_{K_S} \cdot \vec{p}_{K_L}}$$

with

$$E_{K_S} = \sqrt{p_{K_S}^2 + M_K^2} \quad E_{K_L} = \sqrt{p_{K_L}^2 + M_K^2}.$$

On the other hand the collision center of mass energy  $W$  is computed from Bhabha events as described above.

Corrections due to ISR have to be taken into account when relating  $W$  to  $W_{KK}$ . The correction function  $f_K(W)$  has been evaluated using a full detector simulation where

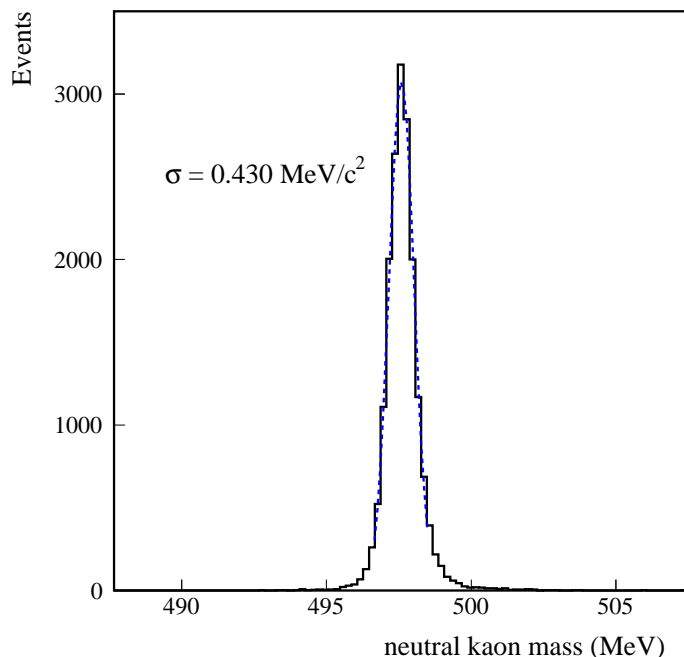


**Figure 3:**  $M_K$  distribution evaluated in a single run of  $\sim 16000$  events from eq. (4.2), the dotted line is a gaussian fit to the peak.

the radiation from both beams has been implemented, and  $W_{KK}$  is reconstructed as in the data. The expression of the radiator function has been taken from ref. [14], including  $\mathcal{O}(\alpha^2)$  corrections. The correction  $|1 - f_K(W)|$  is very small below the resonance, corresponding to a shift in  $W_{KK}$  of 40 keV. For  $W$  above the  $\phi$  mass,  $W_{KK}$  increases up to 100 keV. In this region radiative return begins to be important. The neutral kaon mass is then obtained solving the equation:

$$W = f_K(W) \times W_{KK}(M_K) \tag{4.2}$$

The single event mass resolution is about 430 keV. Contributions to the mass resolution are: experimental resolution about 370 keV, beam energy spread about 220 keV, as measured by KLOE in agreement with machine theory, and ISR about 100 keV. The kaon mass distribution for a single run is shown in figure 3 together with a gaussian fit to the distribution.

The source of systematic errors considered for this measurement are:

1. the momentum calibration;
2. the theoretical uncertainty on the radiator function  $f_K(W)$ ;
3. the absolute calibration of the beam energy.

The systematic error due to the momentum miscalibration has been evaluated by changing the momentum scale in computing the pion momenta. A momentum miscalibration,  $\delta p/p$ , translates to a miscalibration on  $\delta M_K/M_K = 0.06 \delta p/p$ , in agreement with

the qualitative calculation made above. The momentum scale is obtained by using several processes covering a wide momentum range 50 to 500 MeV ( $K_L \rightarrow \pi^+\pi^-\pi^0$ ,  $K_L \rightarrow \pi\nu$ ,  $\phi \rightarrow \pi^+\pi^-\pi^0$ ), with a fractional accuracy below  $2 \times 10^{-4}$ , in agreement with the estimate obtained using Bhabhas [15], resulting in a systematic error  $\delta M_K$  of 6 keV.

The systematic error coming from theoretical uncertainty of the radiator function has been evaluated considering the contribution from higher order terms in  $\alpha$ . The correction function  $f_K(W)$  has been evaluated by excluding the constant term in the  $\mathcal{O}(\alpha^2)$ . The corresponding change in  $f_K(W)$  is  $1.3 \times 10^{-5}$  corresponding to a variation on  $M_K$  of 7 keV. Further checks have been made by using the function given in ref. [16]: no significant differences were observed. Additional systematics come from the dependence of the measured mass from the  $W$  value: we compare the average of the measurements with data collected at  $W < 1020$  MeV with data at  $W > 1021$  MeV, where the value of  $f_K(W)$  is more than a factor two larger. The difference between the two mass values is  $M_K(W < 1020) - M_K(W > 1021) = 9 \pm 10$  keV, consistent with zero.

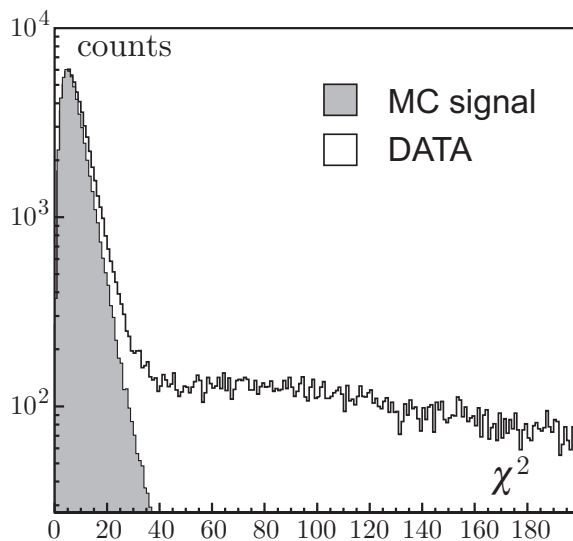
Other sources of systematics are due to the uncertainties on the  $W$  calibration, i.e., the statistic and systematic error on  $M_\phi^{CMD-2}$  and on  $M_\phi$  obtained from our fit. The total contribution from these sources amounts to a mass uncertainty of 15 keV. Systematic uncertainties are treated as uncorrelated. The result is:

$$M_K = 497.583 \pm 0.005_{\text{stat}} \pm 0.020_{\text{syst}} \text{ MeV}. \quad (4.3)$$

## 5. The $\eta$ mass

The decay  $\phi \rightarrow \eta\gamma$ , for  $\phi$ -meson at rest, is a source of monochromatic  $\eta$ -mesons of  $\sim 362.8$  MeV momentum, recoiling against a photon of equal momentum. Detection of such a photon signals the presence of an  $\eta$ -meson. Photons from  $\eta \rightarrow \gamma\gamma$  have a flat spectrum in the range  $147 < E_\gamma < 510$  MeV in the laboratory frame. In the laboratory, the opening angle of the two photons has a distribution peaked at its minimum value of  $113^\circ$ . KLOE measures this angle with an accuracy of  $\sim 0.4^\circ$ . The value of the minimum angle is a function of the  $\eta$  mass and its measurement determines the mass with a resolution of 2 MeV, without energy measurements. In fact we do measure the photon energies. The  $\eta$ -mass accuracy is however ultimately due to the accurate measurement of the photon angles. Together with the stability of the continuously calibrated detector and the very large sample of  $\eta$ -mesons collected we have been able to obtain a very accurate measurement of the  $\eta$ -mass [17].

Events are selected requiring at least three energy clusters in the barrel calorimeter with polar angle  $50^\circ < \theta_\gamma < 130^\circ$ . A kinematic fit imposing energy-momentum conservation is performed. The fitted photon energy resolution is vastly improved over the EMC measurement because of the good angular resolution. The kinematic fit uses the value of the total energy, the  $\phi$  transverse momentum and the average value of the beam-beam interaction point; these values are determined with good precision run by run by analyzing  $e^+e^- \rightarrow e^+e^-$  elastic scattering events. Figure 4 shows the  $\chi^2$  of the kinematic fit for the data and for Monte Carlo [15] simulated signal events. If more than three photons are selected, the combination with the lowest  $\chi^2$  is chosen. Events with  $\chi^2 < 35$  are kept for the analysis.



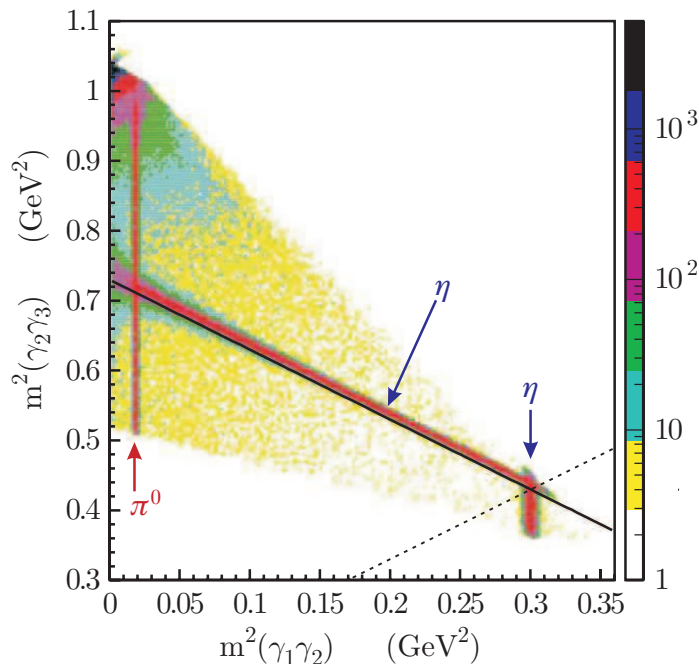
**Figure 4:** Distribution of the  $\chi^2$  of the kinematic fit: dashed area for the MC simulation of  $\phi \rightarrow \pi^0\gamma, \phi \rightarrow \eta\gamma$  events; histogram for data.

Figure 5 shows the  $m_{\gamma_2\gamma_3}^2, m_{\gamma_1\gamma_2}^2$  Dalitz plot population, with the energies ordered as  $E_{\gamma_1} < E_{\gamma_2} < E_{\gamma_3}$ . The  $m_{\gamma_1\gamma_2}^2 \simeq m_{\pi^0}^2$ ,  $m_{\gamma_1\gamma_2}^2 \simeq m_{\eta}^2$  and  $m_{\gamma_1\gamma_3}^2 \simeq m_{\eta}^2$  bands are clearly visible. We apply a cut  $m_{\gamma_1\gamma_2}^2 + m_{\gamma_2\gamma_3}^2 \leq 0.73 \text{ GeV}^2$ , “Dalitz plot cut” in the following, shown by the line in figure 5. Events below the line are retained for the analysis. This allows to select a region of the Dalitz plot with almost no background for the evaluation of the  $\eta$  mass, using just a single cut. The cut also selects events quite symmetric in energy, with all photon energies of  $\mathcal{O}(350)$  MeV. In this way all three cluster positions are determined with good accuracy. The resulting  $m_{\gamma_1\gamma_2}$  distribution, for a fraction of the data, is shown in figure 6, top. The  $m(\gamma_1\gamma_2)$  distribution in the 542.5 to 552.5 interval is fitted well with a single gaussian with  $\sigma = 2.0$  MeV as shown in figure 6, bottom.

To estimate systematic uncertainties we have studied the effects of the detector response and alignment, event selection cuts, kinematic fit and beam energy calibration that can influence our measurement. The values of the systematic errors are summarized in table 1.

First, to check the effect of the  $e^+e^-$  interaction point and the alignment of the calorimeter relative to the drift chamber, we have selected a high purity sample of  $e^+e^- \rightarrow \pi^+\pi^-\gamma$  events [18]. The average position of the interaction point, determined run by run with  $e^+e^- \rightarrow e^+e^-$  events, has been compared with the average position of reconstructed  $\pi^+\pi^-$  vertex. The difference between the two values was computed run by run and the rms of these points ( $\sigma_{\text{vtx}}$ ) was used to evaluate the systematic error introduced in the kinematic fit by varying the IP position by  $\pm 1\sigma_{\text{vtx}}$ . To check for misalignments between the calorimeter and the drift chamber, each pion track was extrapolated to the calorimeter and compared with the centroid of the cluster. A small correction of 1.1 mm along the vertical coordinate,  $y$ , and of 2.0 mm along the longitudinal coordinate,  $z$ , was applied. The rms





**Figure 5:** Population in the  $m_{\gamma_2\gamma_3}^2, m_{\gamma_1\gamma_2}^2$  plane. The photon energies are ordered as  $E_{\gamma_1} < E_{\gamma_2} < E_{\gamma_3}$ . The  $\eta$  and  $\pi^0$  signal are quite evident. Dashed line see text.

( $\sigma_{\text{displ}}$ ) of the mean difference between the coordinates of the extrapolated point and the cluster centroid was used to compute the systematic uncertainty on the  $\eta$  mass by shifting the photon point of arrival at the EMC by  $\sigma_{\text{displ}}$ .

The energy scale of the calorimeter response and its linearity are checked using two different samples of  $e^+e^- \rightarrow \pi^+\pi^-\gamma$  and  $e^+e^- \rightarrow e^+e^-\gamma$  events. The energy of the photon, determined from the track momenta and the average value of  $W$ , was compared with the calorimeter cluster energy. The calorimeter energy scale was calibrated to better than 1% and the response is linear to better than 2% in the range of interest. The systematic effect on the two-photon invariant mass is 4 keV from the energy scale miscalibration and 4 keV from the non-linearity. The values above confirm that the mass measurement has little sensitivity to the calorimeter energy response.

It is however important to check the correctness of the position measurement in the 24 calorimeter modules of the barrel. We compute the two-photon invariant mass for different orientations of the  $\gamma_1\gamma_2\gamma_3$  plane. The rms width of the  $\eta$  mass distribution was assumed as systematic error: 10 keV and 15 keV respectively for variations of the polar and azimuth angle of the normal to the plane.

Systematic effects from event selection criteria were studied by changing the  $\chi^2$  cut (figure 4), showing no influence ( $< 1$  keV) on the result, and the “Dalitz plot cut” of figure 5. The “Dalitz plot cut”, is not parallel to the  $m_{\gamma_1\gamma_2}$  axis. The cut therefore produces an asymmetry in the  $m_{\gamma_1\gamma_2}$  distribution due both to the background and the concentration of the signal in a band perpendicular to the  $m_{\gamma_1\gamma_2}$  axis. The effect of this asymmetry on the

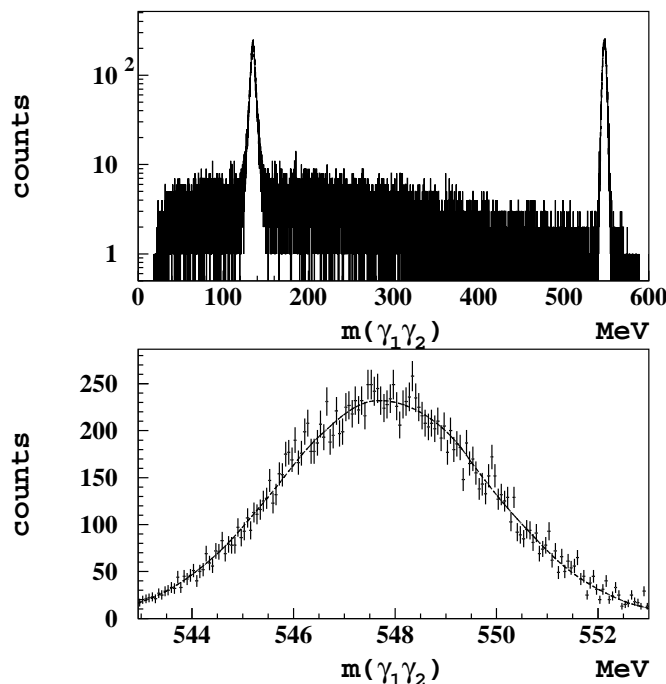


**Figure 6:** Top: Distribution of the invariant mass  $m(\gamma_1\gamma_2)$ , for the events selected by the cut shown in figure 5 Bottom: Distribution of the invariant mass  $m(\gamma_1\gamma_2)$  around the value of the  $\eta$  mass and the gaussian fit. The result of the fit is  $m_\eta = 547.777 \pm 0.016$  MeV with  $\chi^2/\text{n.d.f} = 168/161$ , CL=33%.

measured mass has been studied by translating the straight line cut without rotation as well as changing its slope between -1 and +1 (in steps of 0.5), the last shown in figure 5. In the first case the  $\eta$  mass fluctuates with an rms of 12 keV. In the second case, which clearly brings in a tail at high  $m_{\gamma_1\gamma_2}$ , a systematic shift is observed. This shift has been corrected using a simple MC simulating the observed Dalitz plot population. The mass values, after corrections, fluctuate with an rms of 12 keV. We therefore take the systematic uncertainty due to the cut as 12 keV.

The mass value is very sensitive to the center of mass energy of the  $\eta\gamma$  system used in the kinematic fit. Due to initial state radiation emission (ISR) the available center of mass energy is a bit lower than the value computed from the nominal energy of the  $e^+, e^-$  beams. The effect has been studied with a detailed Monte Carlo simulation of the events in the detector, and a shift of  $\sim 100$  keV was found for the mass measurement. Since this correction is relatively large, we have checked the MC correction due to ISR emission also for runs taken at different values of  $W$ . The data were divided in eight energy bins; moreover, two off-peak energy bins, centered at  $W = 1017$  and  $1022$  MeV, were also analyzed in the same way as the  $\phi$ -peak data. Figure 7, top shows the shift of the mass evaluated by MC as a function of  $W$  together with the measured shift of the  $\eta$  mass respect to the value obtained at  $W = 1019.6$  MeV. Figure 7, bottom shows the value of the mass corrected for the ISR effect. The rms of these points is used as systematic error (8 keV).

The value of the  $\pi^0$  mass was measured with the same method fitting the low mass

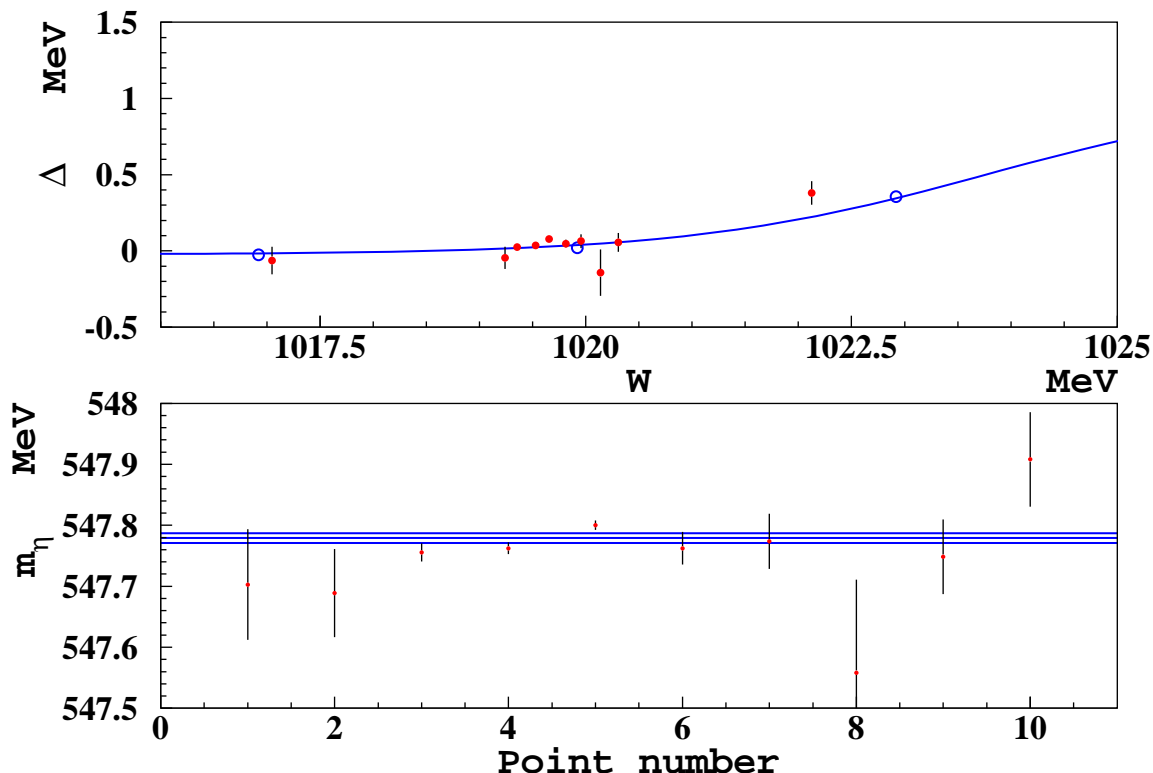


**Figure 7:** Top. Shift of the value of the  $\eta$  mass due to ISR as a function of  $W$ . Open dots: MC, full dots: data ( $m_\eta(W) - m_\eta(1019.6)$ ). The line is a fit to the MC. Bottom. Value of the  $\eta$  mass after the correction as a function of  $W$ . The band corresponds to  $\pm 1\sigma$  around the fitted value.

| Systematic effect           | $m_\eta$ (keV) | $m_{\pi^0}$ (keV) | $R$ ( $\times 10^{-5}$ ) |
|-----------------------------|----------------|-------------------|--------------------------|
| Vertex position             | 4              | 6                 | 19                       |
| Calorimeter energy scale    | 4              | 1                 | 6                        |
| Calorimeter non-linearity   | 4              | 11                | 31                       |
| $\theta$ angular uniformity | 10             | 44                | 120                      |
| $\phi$ angular uniformity   | 15             | 12                | 37                       |
| $\chi^2$ cut                | <1             | 4                 | 13                       |
| Dalitz plot cut             | 12             | 4                 | 18                       |
| ISR emission                | 8              | 9                 | 28                       |
| Total                       | 24             | 48                | 136                      |

**Table 1:** Systematic errors evaluated for  $m_\eta$ ,  $m_{\pi^0}$  and the ratio  $R = m_\eta/m_{\pi^0}$ .

region of figure 6 and the ratio  $R = m_\eta/m_{\pi^0}$  was also determined. All systematic effects discussed above were also evaluated for the mass of the  $\pi^0$  and for the ratio  $R$ ; the corresponding values are listed in table 1.

Finally, the stability of the results as function of running conditions was checked by dividing the data set in eight different periods and determining the values of  $m_\eta$ ,  $m_{\pi^0}$  and

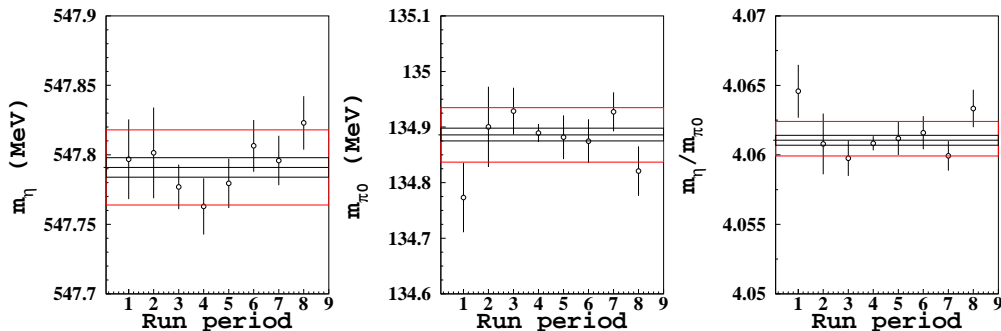


**Figure 8:** Value of the  $\eta$  mass, the  $\pi^0$  mass and of the ratio measured in the eight run periods. The narrow (large) bands correspond to statistical (systematic) error.

$R$  for each period. The results are shown in figure 8 and in table 2 together with their statistical significance. Fits to a common value are good.

|             | Result of the fit      | $\chi^2/\text{d.o.f.}$ | C.L. % |
|-------------|------------------------|------------------------|--------|
| $m_\eta$    | $547,791 \pm 7$ (keV)  | 6.9/7                  | 44 %   |
| $m_{\pi^0}$ | $134,886 \pm 12$ (keV) | 7.7/7                  | 36 %   |
| $R$         | $4.0610 \pm 0.0004$    | 8.9/7                  | 26 %   |

**Table 2:** Result of the fit to the values of  $m_\eta$ ,  $m_{\pi^0}$  and  $R$  in the eight data periods.

The constraint on the total momentum of photons in the kinematic fit is very effective in reducing the error on the two-photon invariant mass. The absolute scale of  $W$  is determined using the CMD2  $m_\phi$  value as in the  $K$  mass measurement section.

Combining the values of table 2 with the scale ratio  $M_\phi^{\text{CMD}}/M_\phi^{\text{KLOE}}=1.00015\pm 0.000029$  we obtain:

$$m_{\pi^0} = (134.906 \pm 0.012_{\text{stat}} \pm 0.049_{\text{syst}}) \text{ MeV} \quad (5.1)$$

$$m_\eta = (547.874 \pm 0.007_{\text{stat}} \pm 0.029_{\text{syst}}) \text{ MeV} \quad (5.2)$$

the  $\pi^0$  mass value is in agreement with the world average [19] within  $1.4\sigma$ .

As a check of this result, we can use the measured ratio  $R$ :

$$\frac{m_\eta}{m_{\pi^0}} = 4.0610 \pm 0.0004_{\text{stat}} \pm 0.0014_{\text{syst}} \quad (5.3)$$

and the world average value of the  $\pi^0$  mass,  $m_{\pi^0} = (134.9766 \pm 0.0006) \text{ MeV}$  [19] to derive  $m_\eta = (548.14 \pm 0.05_{\text{stat}} \pm 0.19_{\text{syst}}) \text{ MeV}$ , consistent with the results quoted above although affected by a larger systematic error due to a worse cluster position reconstruction of the two photons from  $\pi^0$  decays which have a lower energy.

## 6. Conclusions

Our  $K^0$  mass measurement is in acceptable agreement with the previous measurements shown in table 3, but more accurate. Averaging [5, 6] and our result we obtain  $M_{K^0} = 497.610 \pm 0.015 \text{ MeV}$ .

Our measurement of the  $\eta$  mass (eq. (5.2)) is the most accurate result today. It is in good agreement with the recent measurements based on  $\eta$  decays listed in table 4.

| Experiment |     | Method                       | $m_{K^0}$ (MeV)               | events |
|------------|-----|------------------------------|-------------------------------|--------|
| CMD        | [5] | $e^+e^- \rightarrow K_L K_S$ | $497.661 \pm 0.033$           | 3713   |
| NA48       | [6] | $K_L \rightarrow 3\pi^0$     | $497.625 \pm 0.001 \pm 0.031$ | 665 k  |
| KLOE       |     | $e^+e^- \rightarrow K_L K_S$ | $497.583 \pm 0.005 \pm 0.020$ | 35 k   |

**Table 3:** Recent measurements of the  $K^0$  mass.

| Experiment |     | Method   | $m_\eta$ (MeV)                |
|------------|-----|--|-------------------------------|
| GEM, MM    | [1] | $p d \rightarrow {}^3\text{He} \eta$                     | $547.311 \pm 0.028 \pm 0.032$ |
| NA48, IM   | [2] | $\eta \rightarrow 3\pi^0$                                | $547.843 \pm 0.030 \pm 0.041$ |
| CLEO-c, IM | [4] | $\eta \rightarrow \gamma\gamma, 3\pi^0, \pi^+\pi^-\pi^0$ | $547.785 \pm 0.017 \pm 0.057$ |
| KLOE, IM   |     | $\eta \rightarrow \gamma\gamma$                          | $547.874 \pm 0.007 \pm 0.029$ |

**Table 4:** Recent measurement of the  $\eta$ -meson mass. IM stands for invariant mass of decay products, MM for missing mass at production.

Averaging the mass values from [2, 4] and our result we obtain  $m_\eta = 547.853 \pm 0.024$  MeV with a CL of 37%, a value different by  $\sim 12\sigma$  from the average of the measurements done studying the production of the  $\eta$  meson at threshold in nuclear reactions.

## Acknowledgments

We thank the DAFNE team for their efforts in maintaining low background running conditions and their collaboration during all data-taking. We want to thank our technical staff: G.F. Fortugno and F. Sborzacchi for their dedicated work to ensure an efficient operation of the KLOE Computing Center; M. Anelli for his continuous support to the gas system and the safety of the detector; A. Balla, M. Gatta, G. Corradi and G. Papalino for the maintenance of the electronics; M. Santoni, G. Paoluzzi and R. Rosellini for the general support to the detector; C. Piscitelli for his help during major maintenance periods. This work was supported in part by EURODPHNE, contract FMRX-CT98-0169; by the German Federal Ministry of Education and Research (BMBF) contract 06-KA-957; by Graduiertenkolleg ‘H.E. Phys. and Part. Astrophys.’ of Deutsche Forschungsgemeinschaft, Contract No. GK 742; by INTAS, contracts 96-624, 99-37; and by the EU Integrated Infrastructure Initiative HadronPhysics Project under contract number RII3-CT-2004-506078.

## References

- [1] GEM collaboration, M. Abdel-Bary et al., *A precision determination of the mass of the eta meson*, *Phys. Lett.* **B 619** (2005) 281 [[hep-ex/0505006](#)].
- [2] NA48 collaboration, A. Lai et al., *New measurements of the  $\eta$  and  $K^0$  masses*, *Phys. Lett.* **B 533** (2002) 196 [[hep-ex/0204008](#)].
- [3] KLOE collaboration, B. Di Micco et al., *The  $\eta \rightarrow \pi^0\gamma\gamma, \eta/\eta'$  mixing angle and the  $\eta$  mass measurement at KLOE*, *Acta Phys. Slov.* **56** (2006) 403.
- [4] CLEO collaboration, D.H. Miller et al., *Measurement of the  $\eta$ -meson mass using  $\psi_{2s} \rightarrow \eta J/\psi$* , *Phys. Rev. Lett.* **99** (2007) 122002 [[arXiv:0707.1810](#)].

- [5] L.M. Barkov et al., *Precision measurement of the mass of the neutral kaon*, *Yad. Fiz.* **46** (1987) 1088.
- [6] NA48 collaboration, A. Lai et al., *New measurements of the  $\eta$  and  $K_0$  masses*, *Phys. Lett. B* **533** (2002) 196 [[hep-ex/0204008](#)].
- [7] M. Adinolfi et al., *The tracking detector of the KLOE experiment*, *Nucl. Instrum. Meth.* **A488** (2002) 51.
- [8] M. Adinolfi et al., *The KLOE electromagnetic calorimeter*, *Nucl. Instrum. Meth.* **A482** (2002) 364.
- [9] KLOE collaboration, M. Adinolfi et al., *The trigger system of the KLOE experiment*, *Nucl. Instrum. Meth.* **A492** (2002) 134.
- [10] C.M. Carloni Calame, G. Montagna, O. Nicosini and F. Piccinini, *The Babayaga event generator*, *Nucl. Phys.* **131** (*Proc. Suppl.*) (2004) 48 [[hep-ph/0312014](#)].
- [11] KLOE collaboration, F. Ambrosino et al., *Measurement of the DAΦNE luminosity with the KLOE detector using large angle Bhabha scattering*, *Eur. Phys. J. C* **47** (2006) 589 [[hep-ex/0604048](#)].
- [12] CMD-2 collaboration, R.R. Akhmetshin et al., *Measurement of  $\phi$  meson parameters in  $K_L^0 K_s^0$  decay mode with CMD-2*, *Phys. Lett. B* **466** (1999) 385 [*Erratum ibid.* **B 508** (2001) 217] [[hep-ex/9906032](#)].
- [13] CMD-2 collaboration, R.R. Akhmetshin et al., *Reanalysis of hadronic cross section measurements at CMD-2*, *Phys. Lett. B* **578** (2004) 285 [[hep-ex/0308008](#)].
- [14] M. Greco, G. Montagna, O. Nicosini and F. Piccinini, *The second DAΦNE physics handbook* (1995).
- [15] F. Ambrosino et al., *Data handling, reconstruction and simulation for the KLOE experiment*, *Nucl. Instrum. Meth.* **A534** (2004) 403 [[physics/0404100](#)].
- [16] E.A. Kuraev and V.S. Fadin, *On Radiative Corrections to the cross section for single-photon annihilation of an  $e^+e^-$  pair at high energy*, *Sov. J. Nucl. Phys.* **41** (1985) 466 [*Yad. Fiz.* **41** (1985) 733].
- [17] B. Di Micco, *Precise measurement of the  $\eta$  mass*, KLOE note 217 (2007), <http://www.lnf.infn.it/kloe/pub/knote/kn217.ps>.
- [18] KLOE collaboration, A. Aloisio et al., *Measurement of  $\sigma(e^+e^- \rightarrow \pi^+\pi^-\gamma)$  and extraction of  $\sigma(e^+e^- \rightarrow \pi^+\pi^-)$  below 1 GeV with the KLOE detector*, *Phys. Lett. B* **606** (2005) 12 [[hep-ex/0407048](#)].
- [19] PARTICLE DATA GROUP collaboration, W.M. Yao et al., *Review of particle physics*, *J. Phys.* **G 33** (2006) 1.